



# Cooperative Guidance Law for Target Pair to Lure Two Pursuers into Collision

Zheng Wen Tan,\* Robert Fonod,<sup>†</sup> and Tal Shima<sup>‡</sup>  
*Technion—Israel Institute of Technology, 3200003 Haifa, Israel*

DOI: 10.2514/1.G003357

A novel cooperative defensive guidance law is presented for a two-on-two engagement. Instead of classical strategies in which evasive maneuvers are performed or additional agents (e.g., defender missiles) are deployed, the target pair lures the pursuing missiles into collision. The optimal cooperative strategy is solved using state-dependent Riccati equation method. Linearized kinematics and arbitrary-order linear adversaries' dynamics are assumed in the guidance law derivation. Imperfect information is assumed on the relative states and the guidance laws employed by the missile pair. Guidance strategies that the pursuing missiles may employ are assumed to belong to a finite set of linear guidance laws. In addition to the proposed cooperative defensive strategy, a decentralized estimation scheme based on the multiple-model adaptive estimation approach is also presented. Guidance law and estimation performance are demonstrated using nonlinear simulations. Simulation results show the viability of the proposed guidance law and highlight the sensitivity of the guidance law to range measurement accuracy.

## Nomenclature

$A, B, C$	= linearized collision geometry state-space model matrices	$V_C$	= closing speed
$A_v, B_v, C_v, d_v$	= state-space model matrices of the dynamics of vehicle $v$	$v$	= measurement noise
$a$	= acceleration normal to flight-path angle	$X_c^0, Y_c^0$	= initial position coordinates of $c$
$c$	= center of the line of sight between missiles	$\bar{X}_c^0, \bar{Y}_c^0$	= normalized $X_c^0, Y_c^0$
$g$	= gravitational constant	$X_I, Y_I$	= inertial position coordinates
$H$	= measurement matrix	$x$	= state vector for estimation purposes
$K_{MTi}$	= gain matrix for linear guidance law	$x_v$	= state vector representing the dynamics of vehicle $v$
$J$	= cost function	$y$	= relative displacement normal to initial line of sight
$\mathbb{N}$	= set of natural numbers	$y$	= linear system state vector
$\mathcal{N}$	= normal distribution	$y_v$	= component of $x_v$ orthogonal to the associated line of sight
$N'$	= missile guidance gain	$Z_i(0)$	= a priori information of the missile by the $i$ th target
$P_{MTi}$	= covariance matrix of the $i$ th estimator	$z_i$	= measurement vector of the $i$ th target
$P$	= matrix solution to the Riccati equation	$\gamma$	= flight-path angle
$Q$	= matrix of weights on states in running cost	$\Delta$	= time difference between time to missile–missile collision and missile–target collision
$Q_f$	= matrix of weights on states in terminal cost	$\delta, \theta$	= angles between the velocity vector and line of sight of the pursuer and target, respectively
$\mathbb{R}^n$	= set of real numbers of dimension $n$	$\Lambda_i^j$	= $j$ th mode-conditioned likelihood function of the $i$ th estimator
$R_{MTi}$	= noise covariance matrix of measurements of the $i$ th estimator	$\lambda$	= line-of-sight angle
$R$	= matrix of weights on targets' control effort	$\mu_i^j$	= $j$ th regime probability for the $i$ th estimator
$S_i^j$	= covariance matrix of the $j$ th regime-matched filter of the $i$ th estimator	$v_i^j$	= innovations vector of the $j$ th regime-matched filter of the $i$ th estimator
$T_s$	= sampling period	$\xi_{MT}$	= normalized time
$t$	= time	$\rho$	= range
$t_f$	= final time	$\bar{\rho}_{MM}^0$	= normalized $\rho_{MM}^0$
$\mathcal{U}_i$	= set of possible guidance laws considered in the estimator of $i$ th target	$\sigma_{i,\rho}^2, \sigma_{i,\lambda}^2$	= range and line-of-sight angle measurement noise variances of the $i$ th estimator, respectively
$\mathcal{U}_{\text{comb}}$	= set of possible combination of guidance laws considered	$\tau_v$	= first-order lag of vehicle $v$
$u$	= control vector of vehicle group		
$u$	= control input of vehicle		
$V$	= speed		

Received 1 October 2017; revision received 10 February 2018; accepted for publication 12 February 2018; published online 30 April 2018. Copyright © 2018 by the authors. Published by the American Institute of Aeronautics and Astronautics, Inc., with permission. All requests for copying and permission to reprint should be submitted to CCC at [www.copyright.com](http://www.copyright.com); employ the ISSN 0731-5090 (print) or 1533-3884 (online) to initiate your request. See also AIAA Rights and Permissions [www.aiaa.org/randp](http://www.aiaa.org/randp).

\*Graduate Student, Department of Aerospace Engineering; zheng-wen@campus.technion.ac.il.

<sup>†</sup>Postdoctoral Fellow, Department of Aerospace Engineering; robert.fonod@technion.ac.il.

<sup>‡</sup>Professor, Department of Aerospace Engineering; tal.shima@technion.ac.il. Associate Fellow AIAA.

## Subscripts

$M_i$	= $i$ th missile
$MM$	= missile versus missile engagement
$MT_i$	= $i$ th missile versus $i$ th target engagement
$T_i$	= $i$ th target
$v$	= vehicle

## Superscripts

lin	= linear
max	= maximum

NL = nonlinear  
 0 = initial condition  
 \* = optimal

## I. Introduction

MULTIVEHICLE cooperation has received much attention in recent years because it has shown tremendous potential in missions such as wide-area persistent surveillance [1], cooperative tactical reconnaissance [2], and cooperative salvo attack [3]. Although guidance strategies have been developed specifically for the aforementioned missions, limited work has been done to study how cooperation could improve the survivability of such multivehicle teams. This becomes increasingly important as countermeasures, for example in [4], are developed to take down such teams before they could complete their missions. In this paper, the problem of aircraft survivability in a multivehicle engagement is tackled. Specifically, a cooperative defensive strategy is derived for a pair of aircraft (henceforth known as “targets” and abbreviated as “ $T$ ”) being pursued by a pair of missiles (henceforth known interchangeably as “missiles” or “pursuers” and abbreviated as “ $M$ ”).

The classical approach from a target’s perspective in a missile–target engagement is to maximize the miss distance between itself and the missile. Research on optimal target evasion strategies in a one-on-one scenario has been well established. Optimal evasion strategies have been solved using two approaches: 1) by formulating the problem as a pursuit–evasion differential game [5–8], or 2) a one-sided optimal evasion problem. In the latter, the missile guidance strategy is assumed to be known to the target [9–13]. The works in [9–12] studied the optimal evasion problem against a missile using proportional navigation (PN), whereas in [13], optimal evasion strategies were also solved for missiles using augmented PN (APN) and optimal guidance law (OGL).

A key assumption in a one-sided optimal evasion problem is that the target must have exact knowledge of the missile’s guidance strategy. Works such as [14,15] relaxed this assumption by incorporating a multiple-model adaptive estimator (MMAE) to identify the guidance law of the pursuing missile. First pioneered by Magill [16], the MMAE approach is applied on a one-sided optimal evasion problem in [15], where it was assumed that the pursuing missile is employing one of a finite set of linear guidance laws and guidance parameters. Known often as a “mode” or “regime”, each model in the MMAE represents a possible missile guidance law and its corresponding guidance parameter. During the estimation process, the MMAE scheme runs a bank of filters, such as the extended Kalman filter (EKF) used in [15], in parallel with a filter matching each of the possible regimes. Estimation of the system states is obtained by a weighted sum of the state estimates from each filter in the bank, and the weights represent the probability of each regime matching the true guidance strategy of the pursuing missile based on measurement history. Regime probabilities are updated at each time step using Bayesian inference. It is calculated based on the previous time step’s regime probabilities and the regime-conditioned likelihood of the new measurement. One-sided optimal evasion is solved for each of the possible regimes, and the final target maneuver is derived under a multiple-model adaptive control (MMAC) [17] framework. In the MMAC approach, the final evasion command is determined by either the minimum mean-squared error (MMSE) criterion, where the command is a regime probability weighted sum of every optimal maneuver matched to each possible regime, or a maximum a posteriori probability (MAP) criterion, where the latter matches the optimal maneuver against the regime that is most likely to be true.

An alternative target defensive strategy aside from purely evading is to use defender missiles to intercept the pursuer [13,14,18,19]. This strategy is especially advantageous for a target that has a large maneuverability disadvantage over its pursuer, and pursuer–target interception is unavoidable using purely evasive maneuvers. Shaferman and Shima [14] developed a multiple-model adaptive guidance strategy to the three-body problem in which an MMAE is applied to identify the pursuer’s guidance strategy so that the

target–defender team could maneuver optimally to enforce pursuer–defender interception. Besides solving this three-body engagement as a one-sided optimal control problem, different approaches were also proposed by works such as [18,19]. Ratnoo and Shima [18] derived a guidance strategy in which the defender employs line-of-sight (LOS) guidance to maintain its position on the LOS connecting the target platform to the pursuer. Kumar and Shima [19] developed nonlinear guidance strategies based on sliding-mode control techniques and highlighted its effectiveness even if there were large errors in the initial heading and the time-to-go estimates for the defender.

In this paper, we consider the problem of a two-on-two scenario in which the objective of the target pair is to survive the engagement by luring the two pursuers into collision with each other through cooperative maneuvers. This problem, to the best of the authors’ knowledge, has not been explored in open literature. It differs from previous works because the target pair does not simply evade from their pursuers nor do they require additional defender missiles to survive the engagement. The proposed strategy does, however, draw inspiration from the target–defender–pursuer engagement, but instead of luring the pursuers into a defender, the targets capitalize on the presence of multiple adversaries to guide the pursuers into collision with themselves. This multiple-missile engagement also presents an interesting challenge when incorporating the MMAE with the cooperative guidance strategy because the latter is unique to each possible combination of guidance laws employed by the missile pair. If the MMAE problem is solved conventionally, in which each possible combination is modeled by a separate filter in the regime bank, the number of filters will grow quadratically with the number of possible missile guidance laws considered for each missile and can become computationally intensive.

The main contribution of this paper is to present a novel cooperative defensive strategy for the target pair in a two-on-two scenario in which the targets ensure their survivability by luring the pursuing missiles into collision. It is assumed that the pursuers are using one of the finite set of linear guidance laws. The target pair is assumed to know this set but not the active guidance laws being employed by the missiles. The vehicles are assumed to have arbitrary-order linear dynamics. In addition, a decentralized MMAE approach is proposed for state estimation and missile guidance law identification. In this decoupled approach, each target only computes the estimates of states related to its own pursuer and need not account explicitly every possible guidance law combination of the pursuer pair in its regime bank. Although the target pair has imperfect information of the relative states between the missiles and the targets, perfect information of the targets’ positions, accelerations, and flight-path angles are assumed. Communication of the preceding information between the targets is also assumed to occur with zero lag.

The remainder of this paper is organized as follows. Description of the two-on-two engagement and its mathematical model will be presented in Sec. II. Subsequently, the cooperative optimal guidance law of the target pair is derived in Sec. III, and the MMAC-based cooperative guidance strategy is presented in Sec. IV. Detailed analysis of the performance is shown in Sec. V. Finally, some concluding remarks will be made in Sec. VI.

## II. Engagement Formulation

Consider a scenario with two missiles homing on two targets. The objective of the targets in this engagement is to conduct cooperative guidance so that the pursuers are lured into interception with each other without any of the targets being intercepted by the missiles. In addition, we assume that the problem can be simplified to a point-mass planar engagement, and effects of gravity can be neglected. All vehicles use skid-to-turn control with roll stabilization. All vehicles are assumed to have constant speeds and perform lateral maneuvers only. Imperfect information on the relative states between each missile and target is assumed, whereas perfect information on those between the targets is considered. Lag-free communication of all states between the targets is also assumed. Each target in the engagement is assumed to be pursued by one missile, and each

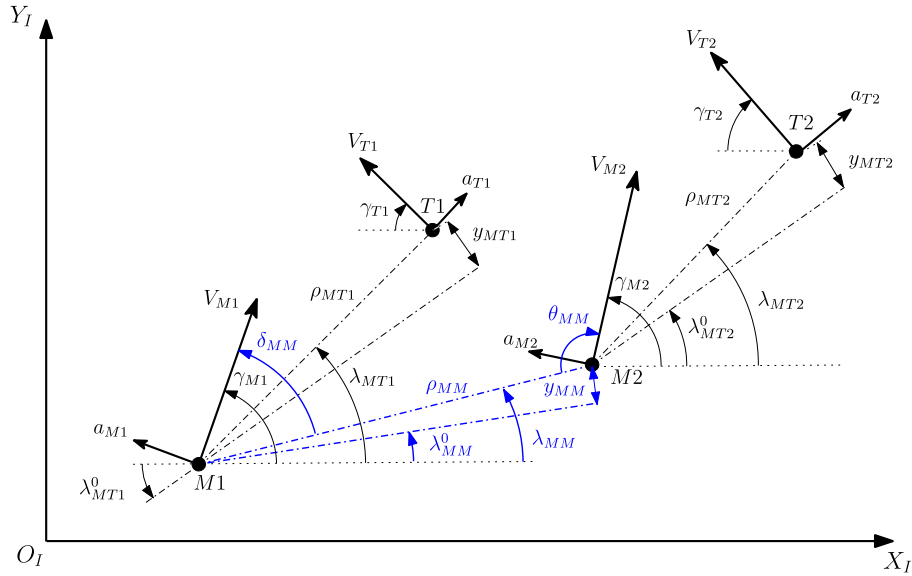


Fig. 1 Schematic of a two-on-two engagement.

missile pursues only one target. The missile pair is also assumed to have no knowledge that they are on a collision course with each other.

A schematic of the engagement can be seen in Fig. 1, where  $X_I-O_I-Y_I$  denotes the Cartesian, inertial reference frame.

### A. Nonlinear Kinematics

Consider first the kinematics of the  $Mi-Ti$  engagement,  $i \in \{1, 2\}$ , in the two-on-two scenario (Fig. 1). Defining the latter in polar coordinates  $(\rho_{MTi}, \lambda_{MTi})$  referenced to  $Mi$ ,  $Ti$ 's state vector of  $Mi$  is

$$\mathbf{x}_{MTi} = [\rho_{MTi} \quad \lambda_{MTi} \quad \mathbf{x}_{Mi} \quad \gamma_{Mi} \quad V_{Mi}]^T \quad (1)$$

where  $\mathbf{x}_{Mi}$  is the internal state vector of  $Mi$  associated with its dynamics. Assuming that the velocity of each vehicle  $v \in \{Mi, Ti\}$  is constant near the end game and their dynamics can be represented by an arbitrary-order linear system, i.e.,

$$\left. \begin{aligned} \dot{\mathbf{x}}_v &= \mathbf{A}_v \mathbf{x}_v + \mathbf{B}_v u_v \\ a_v &= \mathbf{C}_v \mathbf{x}_v + d_v u_v \end{aligned} \right\} \quad (2)$$

the equations of motion (EOMs) associated with  $\mathbf{x}_{MTi}$  are

$$\left. \begin{aligned} \dot{\rho}_{MTi} &= -V_{C,MTi} \\ \dot{\lambda}_{MTi} &= V_{\lambda,MTi}/\rho_{MTi} \\ \dot{\mathbf{x}}_{Mi} &= \mathbf{A}_{Mi} \mathbf{x}_{Mi} + \mathbf{B}_{Mi} u_{Mi} \\ \dot{\gamma}_{Mi} &= a_{Mi}/V_{Mi} \\ \dot{V}_{Mi} &= 0 \end{aligned} \right\} \quad (3)$$

where the closing speed of the  $Mi-Ti$  engagement,  $V_{C,MTi}$ , is

$$V_{C,MTi} = V_{Ti} \cos(\gamma_{Ti} + \lambda_{MTi}) + V_{Mi} \cos(\gamma_{Mi} - \lambda_{MTi}) \quad (4)$$

the speed orthogonal to the  $Mi-Ti$  LOS,  $V_{\lambda,MTi}$ , is

$$V_{\lambda,MTi} = V_{Ti} \sin(\gamma_{Ti} + \lambda_{MTi}) - V_{Mi} \sin(\gamma_{Mi} - \lambda_{MTi}) \quad (5)$$

and  $\gamma_{Ti}$  is defined by the following:

$$\dot{\gamma}_{Ti} = a_{Ti}/V_{Ti} \quad (6)$$

where  $a_{Ti}$  is defined in Eq. (2).

In addition to kinematics between the missiles and targets, the relative motion between  $M1$  and  $M2$  is also described in a manner similar to Eq. (3), i.e.,

$$\left. \begin{aligned} \dot{\rho}_{MM} &= -V_{C,MM} \\ \dot{\lambda}_{MM} &= V_{\lambda,MM}/\rho_{MM} \end{aligned} \right\} \quad (7)$$

where

$$V_{C,MM} = -V_{M2} \cos(\gamma_{M2} - \lambda_{MM}) + V_{M1} \cos(\gamma_{M1} - \lambda_{MM}) \quad (8)$$

$$V_{\lambda,MM} = V_{M2} \sin(\gamma_{M2} - \lambda_{MM}) - V_{M1} \sin(\gamma_{M1} - \lambda_{MM}) \quad (9)$$

### B. Measurement Model

It is assumed that the targets are using electro-optic seekers and/or radar to acquire measurements. Therefore, each target may measure either  $\rho_{MTi}$  and  $\lambda_{MTi}$  or only  $\lambda_{MTi}$ , where  $i \in \{1, 2\}$ . The discrete time measurements  $\mathbf{z}_{MTi}(k) \in \mathbb{R}^{n_z}$  are corrupted by a zero-mean, mutually independent, white Gaussian measurement noise,  $\mathbf{v}_{MTi}(k) \in \mathbb{R}^{n_z}$ . Therefore, the measurement model of the  $i$ th estimator, when both  $\rho_{MTi}$  and  $\lambda_{MTi}$  are available, is

$$\mathbf{z}_{MTi}(k) = \mathbf{H} \mathbf{x}_{MTi}(k) + \mathbf{v}_{MTi}(k) = \begin{bmatrix} \rho_{MTi}(k) \\ \lambda_{MTi}(k) \end{bmatrix} + \mathbf{v}_{MTi}(k) \quad (10)$$

where

$$\mathbf{v}_{MTi}(k) \sim \mathcal{N}([0]_{n_z \times 1}, \mathbf{R}_{MTi}), \quad \mathbf{R}_{MTi} = \text{diag}(\sigma_{i,\rho}^2, \sigma_{i,\lambda}^2) \quad (11)$$

such that  $\mathbf{H}$  is the corresponding measurement matrix, and  $\mathbf{R}_{MTi}$  is the covariance matrix, with  $\sigma_{i,\rho}^2$  and  $\sigma_{i,\lambda}^2$  being the variances for the range and LOS angle measurements acquired by  $i$ th target, respectively. In the case when only  $\lambda_{MTi}$  is acquired, the first row of  $\mathbf{H}$  is removed, and  $\mathbf{R}_{MTi} = \sigma_{i,\lambda}^2$ .

## III. Optimal Cooperative Guidance Law for the Target Pair

In this section, the optimal cooperative guidance law for the target pair is derived. The optimal strategy is solved using linearized kinematics. It is assumed that the missiles are using a linear guidance

law that is known to the target pair through an identification scheme such as the one that will be presented in Sec. IV.A.

### A. Linearized Kinematics for Guidance Law Derivation

Classical linearization [11] about the collision triangles in the engagement is performed with reference to each triangle's initial LOS. The state  $y_{MTi}$ ,  $i \in \{1, 2\}$ , is defined as the separation between  $Mi$  and  $Ti$  orthogonal to the initial LOS of  $Mi$  and  $Ti$ , whereas  $y_{MM}$  is the separation between  $M1$  and  $M2$  orthogonal to the initial LOS of  $M1$  and  $M2$  (Fig. 1).

Because the objective for the target pair defined in this paper is to survive the engagement by cooperatively luring the missiles into collision, the guidance law should drive the final time of the  $M1$ – $M2$  engagement,  $t_{f,MM}$ , to occur earlier than both  $M1$ – $T1$  and  $M2$ – $T2$  engagements, i.e.,

$$t_{f,MM} < \min(t_{f,MT1}, t_{f,MT2}) \quad (12)$$

However, depending on initial positions and flight-path angles of the missiles, condition (12) need not necessarily hold. Referring to Fig. 1, it is evident that, to reduce  $t_{f,MM}$ , the target pair should minimize the magnitude of  $\delta_{MM}$  and  $\theta_{MM}$  so as to increase the closing velocity of the  $M1$ – $M2$  engagement. To this end, the linearized model is formulated incorporating the latter two states.

Thus, to solve for the optimal guidance law, the following linearized state vector  $y$  is defined:

$$y = \left[ y_{MT1}^T \quad y_{MT2}^T \quad y_{MM}^T \quad \delta_{MM} \quad \theta_{MM} \right]^T \quad (13)$$

where

$$y_{MM} = \left[ y_{MM} \quad \dot{y}_{MM} \right]^T, \quad y_{MTi} = \left[ y_{MTi} \quad \dot{y}_{MTi} \quad y_{Mi}^T \quad y_{Ti}^T \right]^T, \quad i \in \{1, 2\} \quad (14)$$

The internal state vectors  $y_{Mi}$  and  $y_{Ti}$  are the components of  $x_{Mi}$  and  $x_{Ti}$  orthogonal to the initial line of sight of the  $Mi$ – $Ti$  engagement and

$$\left. \begin{aligned} \delta_{MM} &\triangleq \gamma_{M1} - \lambda_{MM} \\ \theta_{MM} &\triangleq \pi - (\gamma_{M2} - \lambda_{MM}) \end{aligned} \right\} \quad (15)$$

The linearized EOMs are

$$\dot{y} = \begin{cases} \dot{y}_1 = y_2 \\ \dot{y}_2 = a_{T1}^\perp - a_{M1}^\perp \\ \dot{y}_{M1} = A_{M1} y_{M1} + B_{M1} u_{M1}^\perp \\ \dot{y}_{T1} = A_{T1} y_{T1} + B_{T1} u_{T1}^\perp \\ \dot{y}_{n_{MT1}+3} = y_{n_{MT1}+4} \\ \dot{y}_{n_{MT1}+4} = a_{T2}^\perp - a_{M2}^\perp \\ \dot{y}_{M2} = A_{M2} y_{M2} + B_{M2} u_{M2}^\perp \\ \dot{y}_{T2} = A_{T2} y_{T2} + B_{T2} u_{T2}^\perp \\ \dot{y}_{n_{MT1}+n_{MT2}+5} = y_{n_{MT1}+n_{MT2}+6} \\ \dot{y}_{n_{MT1}+n_{MT2}+6} = -a_{M2}^\perp C_{MM}^\theta / C_{MT2}^\delta - a_{M1}^\perp C_{MM}^\delta / C_{MT1}^\delta \\ \dot{y}_{n_{MT1}+n_{MT2}+7} = \dot{y}_{M1} - \dot{\lambda}_{MM} \\ \dot{y}_{n_{MT1}+n_{MT2}+8} = \dot{\lambda}_{MM} - \dot{y}_{M2} \end{cases} \quad (16)$$

where for  $i \in \{1, 2\}$ ,  $n_{Mi} = \dim(A_{Mi})$ ,  $n_{Ti} = \dim(A_{Ti})$ , and

$$n_{MTi} = n_{Mi} + n_{Ti} \quad (17)$$

and for  $E \in \{MT1, MT2, MM\}$ ,  $\eta \in \{\delta, \theta\}$ ,

$$C_E^\eta = \cos \eta_E \quad (18)$$

with  $\delta_{MTi}$  and  $\theta_{MTi}$  defined as

$$\left. \begin{aligned} \delta_{MTi} &= \gamma_{Mi} - \lambda_{MTi} \\ \theta_{MTi} &= \gamma_{Ti} + \lambda_{MTi} \end{aligned} \right\} \quad (19)$$

and  $\delta_{MM}$  and  $\theta_{MM}$  as presented in Eq. (15).

In Eq. (16), the superscript  $\perp$  represents the component of the acceleration orthogonal to the associated LOS, i.e., for  $i \in \{1, 2\}$ ,

$$a_{Ti}^\perp = a_{Ti} C_{MTi}^\theta \quad (20)$$

$$a_{Mi}^\perp = a_{Mi} C_{MTi}^\delta \quad (21)$$

Assuming that linearization holds,  $\dot{\lambda}_{MM}$  defined in Eq. (7) is incorporated into Eq. (16) in its linearized form as

$$\dot{\lambda}_{MM} = \frac{y_{MM} + \dot{y}_{MM} t_{go,MM}}{V_{C,MM} t_{go,MM}^2} \quad (22)$$

where  $V_{C,MM}$  is defined in Eq. (8), and  $t_{go,MM}$  is defined as

$$t_{go,MM} = t_{f,MM} - t \quad (23)$$

Next, the missiles are assumed to be using a linear guidance law in the following form:

$$u_{Mi}^\perp = K_{MTi} y_{MTi} + K_{u_i} u_{Ti}^\perp \quad (24)$$

where

$$K_{MTi} = \left[ K_1^{Mi} \quad K_2^{Mi} \quad K_{Mi} \quad K_{Ti} \right], \quad i \in \{1, 2\} \quad (25)$$

*Remark 1:* In this paper, the cooperative guidance law is derived against missiles using PN [20], APN [21], and OGL [22]. For the sake of brevity, gains of these well-established linear guidance laws,  $K_{MTi}$  and  $K_{u_i}$ , are not explicitly defined in this paper. Readers are referred to [15] for the detailed formulation of these guidance laws.

Assuming that information about  $K_{MTi}$  and  $K_{u_i}$  is known to the target group, Eq. (16) can be formulated as a one-sided optimal control problem, i.e.,

$$\dot{y} = A(t)y(t) + B(t)u_T(t) \quad (26)$$

such that

$$A(t) = \begin{bmatrix} A_{MT1} & [0] & [0] \\ [0] & A_{MT2} & [0] \\ A_{MM}^{M1} & A_{MM}^{M2} & A_{MM}^0 \end{bmatrix}, \quad B(t) = \begin{bmatrix} B_{MT1} & [0] \\ [0] & B_{MT2} \\ B_{MM}^{T1} & B_{MM}^{T2} \end{bmatrix},$$

$$u_T(t) = \left[ u_{T1}^\perp \quad u_{T2}^\perp \right]^T \quad (27)$$

where  $[0]$  is a matrix of zeros with appropriate dimensions. Elements of  $A(t)$  and  $B(t)$  are defined in Appendix A.

### B. Optimal Cooperative Guidance Law Derivation

As discussed previously, Eq. (12) may not hold for all initial conditions. Thus, to derive a guidance law that can drive the system toward achieving Eq. (12), states  $\delta_{MM}$  and  $\theta_{MM}$  need to be incorporated into the cost function of the optimal control problem.

The cost is defined using the finite-horizon, linear-quadratic formulation:

$$J = \mathbf{y}^T(t_{f,MM}) \mathbf{Q}_f \mathbf{y}(t_{f,MM}) + \int_{t_0}^{t_{f,MM}} [\mathbf{y}^T(t) \mathbf{Q} \mathbf{y}(t) + \mathbf{u}_T^T(t) \mathbf{R} \mathbf{u}_T(t)] dt \quad (28)$$

where

$$\begin{aligned} \mathbf{Q}_f &= \begin{bmatrix} [0] & [0] \\ [0] & \mathbf{w}_f \end{bmatrix}, & \mathbf{w}_f &= \begin{bmatrix} w_{ms} & [0] \\ [0] & [0] \end{bmatrix} \\ \mathbf{Q} &= \begin{bmatrix} [0] & [0] \\ [0] & \mathbf{w}_r \end{bmatrix}, & \mathbf{w}_r &= \begin{bmatrix} w_\delta & 0 \\ 0 & w_\theta \end{bmatrix} \\ \mathbf{R} &= \begin{bmatrix} w_{u1} & 0 \\ 0 & w_{u2} \end{bmatrix} \end{aligned} \quad (29)$$

The weights in Eq. (29) are defined as follows:  $w_{ms}$  is the weight on  $y_{MM}(t_{f,MM})$ ;  $w_\delta$  and  $w_\theta$  are weights on the angles  $\delta_{MM}$  and  $\theta_{MM}$  that were defined in Eq. (15) and shown in Fig. 1; and  $w_{u1}$  and  $w_{u2}$  are weights on  $u_{T1}^\pm$  and  $u_{T2}^\pm$ , respectively.

The objective of the optimal controller,  $\mathbf{u}_T^*(t)$ , is to minimize  $J$  in Eq. (28), i.e.,

$$\mathbf{u}_T^*(t) = \arg \min_{\mathbf{u}_T \in \Omega} J \quad (30)$$

where  $\Omega$  is the set of admissible controls.

The solution to the problem defined in Eq. (30) is given by

$$\mathbf{u}_T^*(t) = -\mathbf{R}^{-1} \mathbf{B}^T(t) \mathbf{P}(t) \mathbf{y}(t) \quad (31)$$

where  $\mathbf{P}(t)$  is the solution to the differential Riccati equation [23]:

$$\begin{aligned} -\dot{\mathbf{P}}(t) &= \mathbf{P}(t) \mathbf{A}(t) + \mathbf{A}^T(t) \mathbf{P}(t) - \mathbf{P}(t) \mathbf{B} \mathbf{R}^{-1} \mathbf{B}^T \mathbf{P}(t) + \mathbf{Q}(t), \\ \mathbf{P}(t_f) &= \mathbf{Q}_f \end{aligned} \quad (32)$$

Physically,  $\mathbf{u}_T^*(t)$  not only minimizes the miss distance between the missiles at  $t_{f,MM}$  with minimal control effort, but it also minimizes the weighted sum of  $\delta_{MM}^2$  and  $\theta_{MM}^2$  over  $[t_0, t_{f,MM}]$  to maximize  $V_{C,MM}$  and drive the missiles to collision before they could hit the targets. Note that this is unlike classical linearization assumptions for missile–target engagements [11] where the geometry of the collision triangle is assumed to be near constant because  $\mathbf{u}_T^*$  is altering the collision geometry at each time step by minimizing  $\delta_{MM}^2$  and  $\theta_{MM}^2$ .

### C. Implementing the Linear Optimal Strategy in the Nonlinear Engagement

The optimal controller,  $\mathbf{u}_T^*$ , in Eq. (31) is solved in the linearized frame and represents the required control that is orthogonal to corresponding line of sight. This subsection describes how  $\mathbf{u}_T^*$  is implemented in the proposed guidance strategy to obtain the nonlinear controller  $\mathbf{u}_T^{\text{NL}}$ .

As noted in Sec. III.B, in such two-on-two engagements, there exist initial conditions in which the missiles are not on the required collision triangle such that the condition in Eq. (12) is met. In such conditions, the targets are required to maneuver in a way such that the initial collision geometry is altered to meet the condition in Eq. (12). Thus, the classical linearization assumption of the collision geometry remaining constant is no longer valid, and to implement the proposed linear controller, this paper employs the state-dependent Riccati equation (SDRE) method [24]. Under the SDRE framework, the nonlinear engagement is relinearized at every time step  $k$ , and Eq. (32) is solved online to obtain  $\mathbf{u}_T^*(k)$ . Finally, to obtain the required nonlinear control at each time step,  $\mathbf{u}_T^{\text{NL}}(k)$ ,  $\mathbf{u}_T^*(k)$  is resolved to the direction orthogonal to the target's velocity vector, i.e.,

$$u_{Ti}^{\text{NL}}(k) = \frac{u_{Ti}^*(k)}{\cos[\gamma_{Ti}(k) + \lambda_{MTi}(k)]}, \quad i \in \{1, 2\} \quad (33)$$

To solve for  $\mathbf{u}_T^*$ , integration of Eq. (32) from  $t_{go,MM} \in [0, t_{f,MM}]$  is required. Because it is assumed that the missile is using classical missile guidance laws, there exist elements that are inversely proportional to  $t_{go,MT1}$  in  $\mathbf{A}(t)$  (see Appendix A), and  $\mathbf{A}(t)$  becomes singular when  $t_{go,MM} = \Delta$ .

In this work, we use the classical linearized method to approximate  $t_{go,E}$  of the collision geometry  $E$ ,  $E \in \{MT1, MT2, MM\}$ , at each time step. Let  $t_{go,E}^{\text{lin}}$  be the linear approximation for the  $t_{go,E}$ ; then,

$$t_{go,E}^{\text{lin}} = \rho_E / V_{C,E}, \quad E \in \{MT1, MT2, MM\} \quad (34)$$

This method of estimating  $t_{go,E}^{\text{lin}}$  can deviate far from the true value especially when there are large changes to the initial collision geometry. Depending on initial conditions, such errors in  $t_{go,E}^{\text{lin}}$  could violate the condition in Eq. (12), although actual values of  $t_{go,E}$  do not. Therefore, for the implementation of the SDRE-based controller in this paper, to avoid the aforementioned singularity issue,  $\bar{t}_{go,MM}$  is used to approximate  $t_{go,MM}$ , where  $\bar{t}_{go,MM}$  is defined by the following conditional statement.

*Condition 1:* If  $t_{go,MM}^{\text{lin}} \neq \min(t_{go,MT1}^{\text{lin}}, t_{go,MT2}^{\text{lin}}, t_{go,MM}^{\text{lin}})$ , then

$$\bar{t}_{go,MM} = \min(t_{go,MT1}^{\text{lin}}, t_{go,MT2}^{\text{lin}}) \quad (35)$$

else

$$\bar{t}_{go,MM} = t_{go,MM}^{\text{lin}} \quad (36)$$

Although Eq. (35) clearly does not accurately depict the true kinematics of the problem, it is a heuristic method that allows us to avoid the singularity problem. It also makes physical sense to assume that the missile–missile collision, if it succeeds, should occur no later than the earliest missile–target collision. Note that although more accurate methods of approximating time to go exists in open literature (e.g., in [25]), the method proposed using condition 1 is much simpler to implement and, as shown in the simulation results in Sec. V, proved to be sufficient for the implementation of the cooperative guidance law.

## IV. Multiple-Model Adaptive-Control-Based Cooperative Guidance Law

In order for the target pair to maneuver optimally against the pursuing missiles and lure them into collision, the targets are assumed to know exactly what guidance laws the missile team is using. In this section, an MMAE approach is proposed to identify the guidance laws employed by the missile team, the relative states of the engagement, and the various time-to-go values necessary for the computation of the cooperative guidance strategy. The section begins with a brief review of the fundamental principles of MMAE before presenting the implementation of the estimator together with guidance law described in Sec. III under an MMAC framework.

### A. Multiple-Model Adaptive Estimator

The MMAE approach [14–16, 26, 27] is a well-established method of estimating unknown system parameters. The system is assumed to have a known finite set of possible regimes, and the true regime is fixed. Filters are run in parallel, and each filter matches one of the possible regimes (see for instance [14]).

In this work, it is assumed that the pursuing missiles are employing one of the  $p$  possible missile guidance strategies in the set  $\mathcal{U}_i$ ,  $i \in \{1, 2\}$ , i.e.,

$$u_{Mi} \in \mathcal{U}_i \triangleq \{u_{Mi}^1, \dots, u_{Mi}^j, \dots, u_{Mi}^p\} \quad (37)$$

In addition, we assume in this paper that the target pair has perfect information on its own parameters associated to the estimation process ( $\mathbf{x}_{Ti}$ ,  $\gamma_{Ti}$ , and  $V_{Ti}$ ,  $i \in \{1, 2\}$ ). It is also assumed that the target pair has exact information on the missile dynamics

(for methods to identify the latter, readers are directed to [14,15]). The estimation process is assumed to be decoupled between the two targets, and the estimator of each target needs only the measurements acquired by itself. Therefore, the  $j$ th regime dynamics is defined by the EOM presented in Eq. (3) with  $u_{Mi} = u_{Mj}^j$  and can be compactly written in discrete time as

$$\mathbf{x}_{MTi}^j(k) = \mathbf{f}_{k-1}^j(\mathbf{x}_{MTi}^j(k-1), \mathbf{u}_T(k-1)), \quad i \in \{1, 2\} \quad (38)$$

where  $\mathbf{x}_{MTi}^j(k)$  is the discretized version of the state vector  $\mathbf{x}_{MTi}(t_k)$  in Eq. (1) associated with the  $j$ th regime and  $t_k = kT_s$ ,  $T_s$  is the sampling period used for estimation. The vector function  $\mathbf{f}_{k-1}^j$  is obtained by integrating the EOMs of the  $j$ th regime from  $t_{k-1}$  to  $t_k$ . In this work, EKF matching the regime dynamics is used to calculate the time update state estimate because the engagement kinematics is nonlinear.

Next, using Bayes's rule, the  $j$ th regime probability at the  $k$ th time step,  $\mu_i^j(k)$ , can be determined by the following recursive formula [26], based on a given initial probability,  $\mu_i^j(0)$ :

$$\mu_i^j(k) = \frac{\Lambda_i^j(k)\mu_i^j(k-1)}{\sum_{l=1}^p \Lambda_i^l(k)\mu_i^l(k-1)}, \quad j \in \{1, \dots, p\} \quad (39)$$

where  $\Lambda_i^j(k) \triangleq f_p(z_i(k)|z_i(1:k-1), u_{Mi}^j)$  is the  $j$ th regime-conditioned likelihood function computed based on the innovations process statistics of the  $j$ th filter of the  $i$ th missile;  $z_i(1:k)$  is the measurement acquired by the  $i$ th missile from first time step to the  $k$ th; and  $f_p(\mathcal{A}|\mathcal{B})$  is the conditional probability density function of  $\mathcal{A}$  given  $\mathcal{B}$ .

Under linear Gaussian assumptions,  $\Lambda_i^j(k)$  is also Gaussian and is thus

$$\Lambda_i^j(k) = \mathcal{N}(\nu_i^j(k); [0]_{n_z \times 1}, \mathbf{S}_i^j(k)) \quad (40)$$

where  $\nu_i^j(k)$  and  $\mathbf{S}_i^j(k)$  are the innovation and its covariance from the  $j$ th regime-matched filter.

### B. Multiple-Model Adaptive Estimator for Identification of Classical Guidance Laws

In this work, the cooperative targets guidance law is derived against a missile team using the well-established classical guidance laws PN, APN, and OGL. Application of these guidance laws is usually in its nonlinear form rather than the linearized formulation presented in Eq. (24). For the sake of brevity, the index for the  $i$ th missile or target,  $i \in \{1, 2\}$ , is dropped in the formulation of this subsection:

$$u_M^j = N'_{GL} \frac{Z_{GL}}{t_{go,MT}^2 \cos(\gamma_M - \lambda_{MT})} \quad GL \in \{PN, APN, OGL\} \quad (41)$$

where  $N'_{GL}$  is the effective navigation gain, and  $Z_{GL}$  is the missile's ZEM distance, which is unique for each guidance law:

$$Z_{PN} = V_{C,MT} \dot{\lambda}_{MT} t_{go,MT}^2 \quad (42a)$$

$$Z_{APN} = Z_{PN} + \frac{t_{go,MT}^2}{2} a_T^\perp \quad (42b)$$

$$Z_{OGL} = Z_{APN} - a_M^\perp t_M^2 \psi(\xi_{MT}) \quad (42c)$$

where  $\dot{\lambda}_{MT}$  and  $V_{C,MT}$  are defined in Eqs. (3) and (4), respectively. Variables  $a_T^\perp$  and  $a_M^\perp$  are the components of the target and missile accelerations orthogonal to the missile-target LOS as presented in Eqs. (20) and (21). And  $\psi(\xi)$  is defined as

$$\psi(\xi_{MT}) = \exp(-\xi_{MT}) + \xi_{MT} - 1 \quad (43)$$

where  $\xi_{MT} \triangleq t_{go,MT}/\tau_M$  is the nondimensionalized time to go.

Although  $N'_{GL}$  are constants for PN and APN,  $N'_{OGL}$  is a function of  $\xi_{MT}$  and is defined as

$$N'_{OGL} = \frac{6\xi_{MT}^2 \psi(\xi_{MT})}{3 + 6\xi_{MT} - 6\xi_{MT}^2 + 2\xi_{MT}^3 - 3\exp(-2\xi_{MT}) - 12\xi_{MT}\exp(-\xi_{MT})} \quad (44)$$

Thus, to determine the guidance law of the missiles, the MMAE is required to identify the ZEM values, Eq. (42), and in the case of PN and APN,  $N'_{GL}$ .

### C. Estimating the Range and Line-of-Sight Angle Between M1 and M2

Besides the states associated with the missile-target collision geometries, the cooperative guidance law defined in Sec. III requires also the states  $\rho_{MM}$  and  $\lambda_{MM}$  for computation of the linearized states. In this work, these states are computed separately out of the estimation loop using the estimates of  $\rho_{MTi}$  and  $\lambda_{MTi}$ ,  $i \in \{1, 2\}$ , and the relative position of the targets. This way, estimation can be decoupled between the targets, and they need only compute the number of filters that corresponds to the  $p$  number of possible guidance laws. Let  $\rho_{TT}$  and  $\lambda_{TT}$  (see Fig. 2) define the relative position between the targets in polar coordinates, and assume that we have perfect information on these parameters. Then, by taking reference from one of the targets, say  $T1$ ,  $\rho_{MM}$  and  $\lambda_{MM}$  can be computed:

$$\left. \begin{aligned} \rho_{MM} &= \sqrt{\Delta X_{MM}^2 + \Delta Y_{MM}^2} \\ \lambda_{MM} &= \arctan(\Delta Y_{MM}/\Delta X_{MM}) \end{aligned} \right\} \quad (45)$$

where

$$\Delta X_{MM} = \rho_{TT} \cos \lambda_{TT} - \rho_{MT2} \cos \lambda_{MT2} + \rho_{MT1} \cos \lambda_{MT1} \quad (46)$$

$$\Delta Y_{MM} = \rho_{TT} \sin \lambda_{TT} - \rho_{MT2} \sin \lambda_{MT2} + \rho_{MT1} \sin \lambda_{MT1} \quad (47)$$

Estimates  $\hat{\rho}_{MM}$  and  $\hat{\lambda}_{MM}$  can then be computed using Eqs. (45–47) based on the estimates  $\hat{\rho}_{MT1}$ ,  $\hat{\rho}_{MT2}$ ,  $\hat{\lambda}_{MT1}$ , and  $\hat{\lambda}_{MT2}$  and variables  $\rho_{TT}$  and  $\lambda_{TT}$ , of which we assumed to have perfect information.

*Remark 2:* If the estimation process is coupled between  $T1$  and  $T2$ , i.e.,  $\rho_{MM}$  and  $\lambda_{MM}$  are estimated by incorporating their dynamics [Eq. (7)] into the EKF equations, then the number of filters increases drastically with  $p$  because, in addition to the number of possible guidance laws employed by each missile, the MMAE scheme has to compute  $p^2$  number of filters in parallel to account for the possible combinations of guidance laws employed by the two missiles. Also, the size of the covariance matrix to be solved by each filter increases

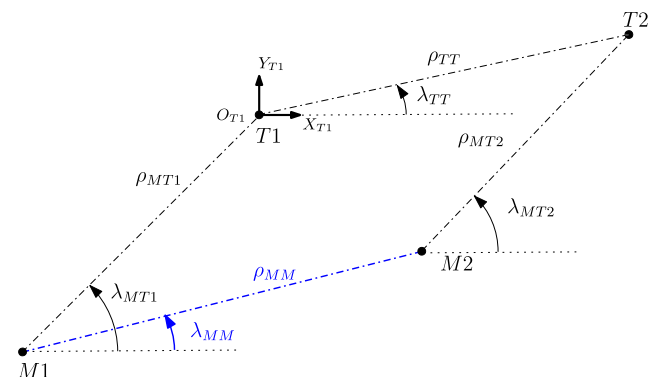


Fig. 2 Relative positions of M1 and M2 referenced to T1.

from  $5 \times 5$  (five states for each  $Mi-Ti$  engagement,  $i \in \{1, 2\}$ ) to  $12 \times 12$  (10 states for both  $Mi-Ti$  engagements plus  $\rho_{MM}$  and  $\lambda_{MM}$ ). This can become very computationally intensive with increasing  $p$ .

**D. Multiple-Model Adaptive-Control-Based Cooperative Guidance Law**

To compute the maneuver commands for the target pair when information on the missiles is imperfect, this paper employs the MMAC approach [17]. In this approach, the state estimates from each filter are fed into a regime-matched controller. The final target commands can then be computed by either 1) minimum mean-squared error (MMSE), or 2) maximum a posteriori probability (MAP) approach.

*1. Minimum Mean-Squared Error Approach*

In the MMSE approach, the final target command  $u_T$  is determined by a weighted average of the regime-matched target commands. However, each regime-matched controller varies with different combinations of guidance laws used by the missile team, and computing the final target commands using the MMSE approach would require multiple solutions of the Riccati equation [Eq. (32)] each accounting for every possible combination.

Consider that each target  $Ti$  computes  $p$  number of regimes that corresponds to the list of possible guidance laws employed by its pursuer  $Mi$ . Let  $\mathcal{U}_{comb}$  denote the set that consists of all possible combinations of guidance laws between  $M1$  and  $M2$ , and  $u_M^l$  is the  $l$ th combination in this set, i.e.,

$$u_M^l = [u_{M1}^{j1}, u_{M2}^{j2}], \quad l \in \{1, \dots, p^2\}, \quad j1, j2 \in \{1, \dots, p\}, \quad \text{and} \quad u_M^l \in \mathcal{U}_{comb} \quad (48)$$

If  $\mathcal{U}_{comb}$  is arranged in the following order:

$$\mathcal{U}_{comb} \triangleq \begin{Bmatrix} u_M^1 \triangleq [u_{M1}^1, u_{M2}^1]^T, \dots, u_M^p \triangleq [u_{M1}^p, u_{M2}^p]^T \\ u_M^{p+1} \triangleq [u_{M1}^2, u_{M2}^1]^T, \dots, u_M^{2p} \triangleq [u_{M1}^p, u_{M2}^p]^T \\ \vdots \\ u_M^{(p-1)p+1} \triangleq [u_{M1}^p, u_{M2}^1]^T, \dots, u_M^{p^2} \triangleq [u_{M1}^p, u_{M2}^p]^T \end{Bmatrix} \quad (49)$$

then the index  $l$  can be written as a function of  $j1$  and  $j2$ :

$$l = (j1-1)p + j2 \quad (50)$$

The combined regime probability of  $u_M^l$  at time step  $k$ ,  $\mu^l(k)$ , is calculated based on the regime probabilities associated with the  $j1$ th and  $j2$ th regimes in the MMAE of  $T1$  and  $T2$ , i.e.,

$$\mu^l(k) = \mu_1^{j1}(k)\mu_2^{j2}(k), \quad l \in \{1, \dots, p^2\} \quad (51)$$

The final command at time step  $k$  in a MMSE sense is

$$u_T^{(mmse)} = \sum_{l=1}^{p^2} \mu^l(k)u_T^{*l} \quad (52)$$

where  $u_T^{*l} = [u_{T1}^{*l}, u_{T2}^{*l}]^T$ ,  $l \in \{1, \dots, p^2\}$ , is the optimal maneuver based on the cooperative guidance strategy as formulated in Sec. III against the  $l$ th combination of missile guidance laws.

*Remark 3:* If the estimation is coupled, then both MMAE scheme and Riccati equation (32) will be computed  $p^2$  number of times in parallel. Instead of Eq. (51),  $\mu^l(k)$  will simply correspond to regime

probability of the  $l$ th regime in the  $p^2$  number of filters in the coupled MMAE scheme.

*2. Maximum A Posteriori Probability Approach*

In the MAP approach,  $u_T$  is determined as the command against the combination of missile guidance laws that has the maximum a posteriori probability. In this approach, only one solution to Eq. (32) is required because we only need to compute the SDRE controller for the combination of guidance laws that corresponds to the regimes with the highest probability from each target's MMAE. Consider the following:

$$\left. \begin{aligned} j1 &= \arg \max_{j \in \{1, \dots, p\}} \mu_1^j(k) \\ j2 &= \arg \max_{j \in \{1, \dots, p\}} \mu_2^j(k) \end{aligned} \right\} \quad (53)$$

then

$$u_T^{(map)} = u_T^{*l} \quad (54)$$

where  $l$  relates to indices  $j1$  and  $j2$  through Eq. (50), and it is the index in  $\mathcal{U}_{comb}$  as defined by Eq. (49).

*Remark 4:* If the estimation process is coupled, then a total of  $p^2$  number of filters need to be run in parallel. However, unlike in MMSE approach,  $u_T^{(map)}$  only needs Eq. (32) to be solved once at each time step for  $u_T^{*l}$  instead of solving all  $p^2$  number of regime-matched optimal maneuvers as shown in Eq. (52).

**E. Sensitivity of Guidance Law to Estimation Performance**

The cooperative guidance law derived in Sec. III follows a similar geometric rule to the classical PN in which collision is achieved if the associated vehicles are able to remain on the collision triangle. The targets must therefore ensure that the LOS rate between the missiles is nullified towards the end of the engagement. Hence, accuracy of the estimate for the LOS angle between the missiles,  $\lambda_{MM}$ , becomes paramount to achieving good miss-distance performance. Figure 3 depicts the effects of missile-target estimation errors on the estimation

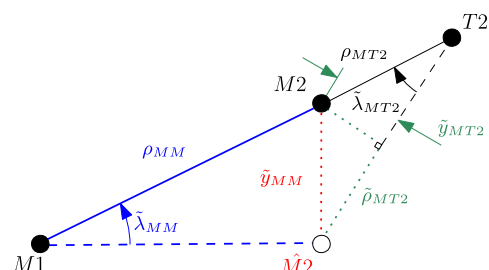


**Fig. 3** Effects of missile-target estimation errors on missile-missile miss-distance estimation  $\tilde{y}_{MM}$ .

**Table 1** Missile–missile miss distance due to estimation errors from missile–target engagement

Case	$\tilde{\lambda}_{MT2}$ , mrad	$\tilde{\rho}_{MT2}$ , m	$\tilde{y}_{MT2}$ , m	$\tilde{y}_{MM}$ , m
Nominal	0.25	1.5	0.5	1.581
$0.1 \times \tilde{\lambda}_{MT2}$	0.025	1.5	0.05	1.501
$0.1 \times \tilde{\rho}_{MT2}$	0.25	0.15	0.5	0.522

error of  $\lambda_{MM}$ . Here, the accent “ $\sim$ ” denotes the estimation error of the associated parameter. For the purpose of this discussion, it is assumed that states of  $M1$  are known perfectly, and  $\tilde{\lambda}_{MM}$  is attributed to errors in state estimates of the  $M2$ – $T2$  engagement. We introduce another parameter in this discussion,  $\tilde{y}_{MM}$ , which represents the difference in the true and estimated position of  $M2$ . The parameter  $\tilde{y}_{MM}$  can also be viewed as the miss distance associated with estimation error,  $\tilde{\lambda}_{MM}$ . Assuming that estimation errors are small near the end of  $M1$ – $M2$  engagement, using small-angle approximations,  $\tilde{y}_{MM}$  can be written as

$$\tilde{y}_{MM} \approx \rho_{MM} \tilde{\lambda}_{MM} = \sqrt{\tilde{y}_{MT2}^2 + \tilde{\rho}_{MT2}^2} \quad (55)$$

such that

$$\tilde{y}_{MT2} \approx \rho_{MT2} \tilde{\lambda}_{MT2} \quad (56)$$

From Eqs. (55) and (56), it is clear that contribution of  $\tilde{\lambda}_{MT2}$  to  $\tilde{y}_{MM}$  diminishes as the range between the  $M2$  and  $T2$  decreases. Assuming that  $\tilde{\lambda}_{MT2}$  and  $\tilde{\rho}_{MT2}$  converge to its asymptotic values toward the end of the engagement and  $\dot{\rho}_{MT2} < 0$ , the influence of  $\tilde{\lambda}_{MT2}$  on  $\tilde{y}_{MM}$  reduces as compared to  $\tilde{\rho}_{MT2}$  as the missile approaches the target. Thus, the quality of the range estimate between the missile and the target becomes the dominant factor influencing the cooperative guidance law’s miss distance performance.

To have some quantitative assessment on the influence of errors in range and LOS angle estimates between the missiles and targets toward  $\tilde{y}_{MM}$ , we compute and tabulate  $\tilde{y}_{MM}$  in Table 1 using Eq. (55) for various error levels in the missile–target state estimates for the case when  $\hat{\rho}_{MT2} = 2000$  m at  $t_{f,MM}$ . Here, it is assumed that the missiles have a nonzero miss (i.e.,  $\rho_{MM} \neq 0$ ) at  $t_{f,MM}$ .

As seen in Table 1, a significant reduction in  $\tilde{y}_{MM}$  is achieved for a given  $\rho_{MM}$  only in the case when  $\tilde{\rho}_{MT2}$  is reduced. This influence of the range estimation accuracy between the missile–target on  $\tilde{y}_{MM}$  will be further validated in the Monte Carlo studies in Sec. V.B.3.

## V. Simulation Analysis

In this section, the performance of the cooperative target guidance strategy derived in Sec. II is presented. The section begins by evaluating the proposed guidance law using perfect information, where we demonstrate the importance of the weights on  $\delta_{MM}$  and  $\theta_{MM}$  in the cost function [Eq. (28)]. A “collision map” is presented thereafter in which the ability of the target team to lure the missile into collision based on different initial conditions is shown.

In the subsequent subsection, performance of the guidance law using the estimated states (i.e., “estimation in the loop”) is analyzed in Monte Carlo (MC) simulations. Results from a sample run are also presented in this subsection to demonstrate the performance of the estimator. Sensitivity of the cumulative distribution function (CDF) of the missile–missile miss distance to measurement noise is also evaluated.

### A. Guidance Law Performance with Perfect Information

#### 1. Simulation Setup

The simulation setup is as follows. All vehicles have constant speeds:  $V_{M1} = V_{M2} = 600$  m/s,  $V_{T1} = V_{T2} = 400$  m/s. Flight-path angles were set such that  $\gamma_{T1} = \gamma_{T2} = 0$  deg, and missiles have zero initial heading error. The guidance laws for  $M1$  and  $M2$  are APN, with  $N'_{APN} = 5$ , and OGL, respectively. All vehicles have

first-order dynamics with time lag constants  $\tau_M = 0.25$  s for both missiles and  $\tau_T = 0.5$  s for both targets. Accelerations were bounded at  $a_T^{\max} = 10$  g for both targets and at  $a_M^{\max} = 20$  g for both missiles, where  $g = 9.80665$  m/s<sup>2</sup> is the gravitational constant. Control update frequency is set at 50 Hz. Unless otherwise stated, weights on the cost function [Eq. (28)] are set as such:  $w_{ms} = 1e4$ ,  $w_{u1} = w_{u2} = 0.003$ , and  $w_\delta = w_\theta = 30$ .

#### 2. Influence of Weights on Guidance Performance

In this subsection, the weights on  $\delta_{MM}$  and  $\theta_{MM}$  from the cost function [Eq. (28)],  $w_\delta$  and  $w_\theta$ , respectively, are varied to demonstrate its influence on the guidance performance. Referring to Fig. 4, when  $w_\delta = w_\theta = 0$ , the targets simply maneuver to minimize the change in LOS between the missiles, through minimizing  $y_{MM}(t_{f,MM})$  in the linear system. Although the targets were able to guide the missiles to be on a collision course, they were not able to do so before  $M2$  collided with  $T2$ . When  $w_\delta = w_\theta = 30$ , the targets maneuver to reduce  $\delta_{MM}$  and  $\theta_{MM}$ , thus driving the missiles to collide at an earlier time. It is important to note that the weights were tuned to ensure zero miss between the missiles; values too high compared to the weight on  $y_{MM}(t_{f,MM})$  will result in nonzero miss, whereas values too low (similar to  $w_\delta = w_\theta = 0$ ) lead to collision between missile(s) and target(s).

*Remark 5:* In the proposed guidance law, collision avoidance between the targets is not explicitly accounted for. Thus, in the singular cases (e.g., when the engagement has perfect symmetry, i.e., in position, target/missile velocities, missile guidance laws), the targets may collide before the missiles do. To avoid target–target collision, the target pair can 1) fly in an asymmetric formation as shown in Fig. 4, 2) fly at different velocities and/or 3) implement an anticollision guidance strategy.

#### 3. Collision Map

The performance of the guidance law is evaluated over a range of initial conditions and presented in a collision map. Missile and target parameters are the same as described in Sec. V.A.1. Target positions are fixed at the same location as seen in Fig. 4, whereas positions of the missiles are varied.

Positions of the missiles are varied as follows. Referring to Fig. 5, the missiles’ initial LOS angle is fixed at  $\lambda_{MM}^0 = -\pi/2$  (i.e., parallel to the  $Y_I$  axis). The center of missile–missile LOS is denoted as  $c$ , and the initial inertial position of  $c$  is  $(X_c^0, Y_c^0)$ . The initial range between the missiles  $\rho_{MM}^0$  together with  $X_c^0$  and  $Y_c^0$  are varied over the intervals  $\rho_{MM}^0 \in [100, 6000]$  m,  $X_c^0 \in [-10000, -1000]$  m, and  $Y_c^0 \in [-3000, 3000]$  m. These parameters are normalized by the initial range between the targets,  $\rho_{TT}^0$ , and are denoted as  $\bar{\rho}_{MM}^0$ ,  $\bar{X}_c^0$ , and  $\bar{Y}_c^0$ , i.e.,

$$\bar{\rho}_{MM}^0 \triangleq \rho_{MM}^0 / \rho_{TT}^0, \quad \bar{X}_c^0 \triangleq X_c^0 / \rho_{TT}^0, \quad \bar{Y}_c^0 \triangleq Y_c^0 / \rho_{TT}^0 \quad (57)$$

The collision maps obtained from the simulations are presented in Fig. 6, in which initial conditions that resulted in missile–missile collision are marked with circles, whereas conditions which led to a miss are marked by asterisks. Missiles are considered to have “collided” if  $\rho_{MM}(t_{f,MM}) \leq 0.1$  m.

As shown in Fig. 6, the guidance law is most effective when  $\bar{\rho}_{MM}^0 > 1$ ,  $\bar{X}_c^0$  is large, and  $\bar{Y}_c^0$  is small. This is intuitive; as observed in the sample trajectory in Fig. 4, the targets require sufficient initial separation between themselves and the missiles so that the target pair has sufficient time to lure the pursuers into collision. The guidance is less effective when  $\bar{\rho}_{MM}^0 < 1$  (i.e.,  $\rho_{MM}^0 < \rho_{TT}^0$ ). In such scenarios, the missile velocities are initially pointing away from each other (because we assumed that the missiles have zero initial heading error), and with decreasing  $\bar{X}_c^0$ , the initial difference between the missile headings becomes too large for the target pair to turn the missiles into head-on collision before one of the targets is intercepted. Also, as seen in Figs. 6c and 6d, the targets were able to enforce collision if  $\bar{Y}_c^0 \sim [-1, 2]$ . This is also intuitive because a large offset in the center point  $c$  meant that one of the missiles is closer to the target than the

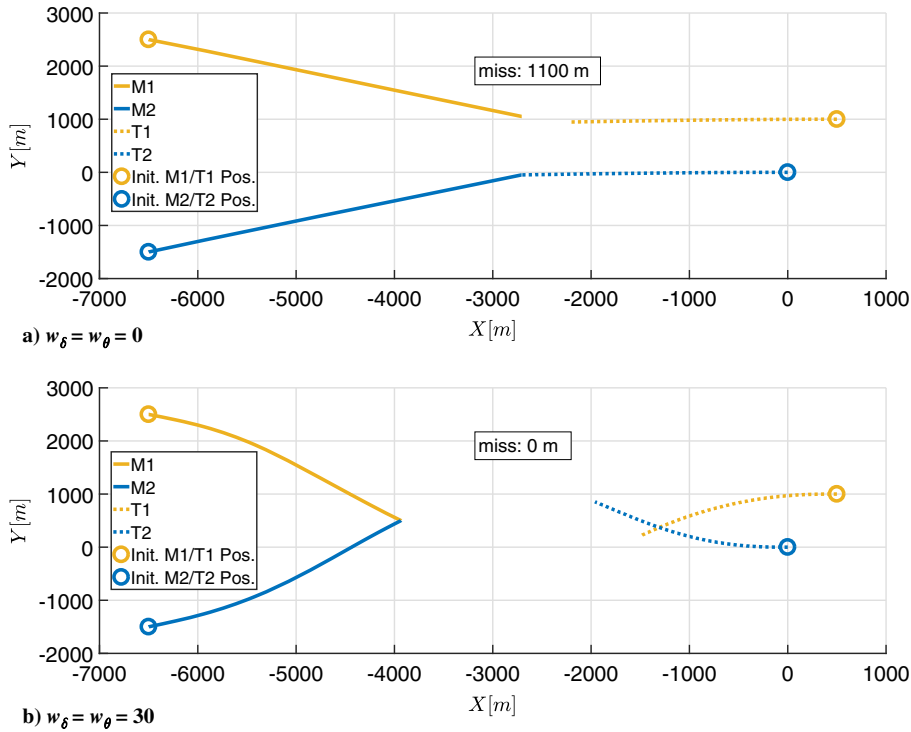


Fig. 4 Influence of the weights on the relative angles between missiles' heading and the LOS between them.

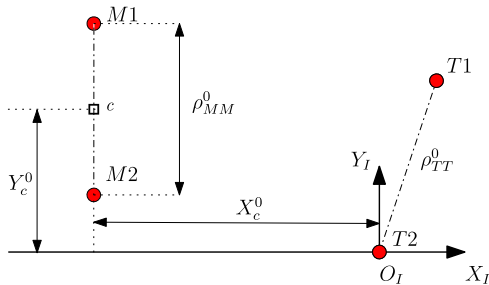


Fig. 5 Relative positions of  $M1$  and  $M2$  referenced to  $T1$ .

other, and target interception would occur earlier than the missile–missile collision.

**B. Monte Carlo Study with Estimator in the Loop**

*1. Simulation Setup*

A Monte Carlo study was conducted to evaluate the estimator-in-the-loop performance of the cooperative guidance law. Inertial positions are the same as that shown in Fig. 4 and are fixed in this study. Initial flight-path angles of the targets are uniformly selected from the interval  $[-10, 10]$  deg, whereas the initial heading errors of the missiles are drawn from a zero-mean normal distribution with 3 deg standard deviation. The guidance law that is employed by each missile is assumed to be one of the seven regimes considered by each target in this study. This includes PN, APN, and OGL with  $N'_{GL} \in \{3, 4, 5\}$  for  $GL \in \{PN, APN\}$ . Selection of the missiles' guidance laws at the beginning of each run is based on the initial regime probability,  $\mu_i^j(0)$ ,  $i \in \{1, 2\}$ ,  $j \in \{1, \dots, 7\}$ .  $\mu_i^j(0)$  is set such that each type of guidance law has 1/3 probability, and each  $N'_{GL}$  has a 1/9 chance of occurring within the guidance law. Each MC simulation includes 500 runs.

In this study, the MAP approach is employed for MMAC (see Sec. IV.D.2) because it is computationally more efficient and is more practical to implement on the onboard processor of an aircraft/missile. Each filter of the  $i$ th estimator is initiated with the same state estimate,  $\hat{x}_{MTi}^j(0|0) \sim \mathcal{N}(x_{MTi}(0), P(0|0))$ ,  $i \in \{1, 2\}$ ,  $j \in \{1, \dots, 7\}$ , where

$x_{MTi}(0)$  is the true initial state, and the initial covariance  $P(0|0) = \text{diag}\{650^2, (3\pi/180)^2, (5g)^2, (3\pi/180)^2, 60^2\}$ .

The targets are assumed to be acquiring both range and bearing measurements that are corrupted by noises as defined in Eq. (11). Variances of the measurement noises are varied in this study to assess the sensitivity of the cooperative guidance law to noise. Measurements are taken at a frequency of 50 Hz.

*2. Sample Run*

A sample run is presented here to demonstrate the performance of the estimator and the guidance law when using imperfect information. In this sample run,  $\sigma_\rho = 10$  m and  $\sigma_\lambda = 1$  mrad. Missile and target parameters follow exactly as described in Sec. V.A.1.

Convergences of the regime probabilities  $\mu_1^j$  and  $\mu_2^j$  are shown in Fig. 7. As seen in the figure, regime probabilities for both missiles converged to 1 by  $t = 4$  s. Convergence of  $\mu_2^j$  is slower because the guidance behaviors for OGL and APN,  $N'_{APN} = 3$  (i.e., the optimal guidance gain for APN), are very similar. They differ only in the term associated with the  $M2$ 's first-order lag,  $\tau_{M2}$  [see Eq. (42)], and because the  $\tau_{M2} = 0.25$  s contribution from this term is hardly discernible. Although this is true,  $T2$ 's estimator correctly identified OGL as the most probable guidance law being employed by  $M2$  throughout the engagement, and because it is using the MAP approach to derive its optimal maneuver, it is still behaving optimally against  $M2$ .

For brevity, only the estimation performance of the states relating to the  $M2$ – $T2$  and  $M1$ – $M2$  engagements are presented because similar results are seen in the  $M1$ – $T1$  case. Despite the slower convergence in the regime probabilities in  $T2$ 's estimator, the state estimation errors converge to their asymptotic values at around 2 s, as seen in Fig. 7. Note that because  $\hat{\rho}_{MM}$  and  $\hat{\lambda}_{MM}$  are computed using Eq. (45) and not within the estimator, only the sample errors without the variances are shown in Fig. 8. For other estimates presented in Fig. 7, the error performance is obtained based on the blended estimate  $\hat{x}_{MTi}$  and blended covariance  $P_{MTi}$  and are calculated using

$$\hat{x}_{MTi}(k|k) = \sum_{j=1}^p \mu_i^j(k) \hat{x}_{MTi}^j(k|k) \tag{58a}$$

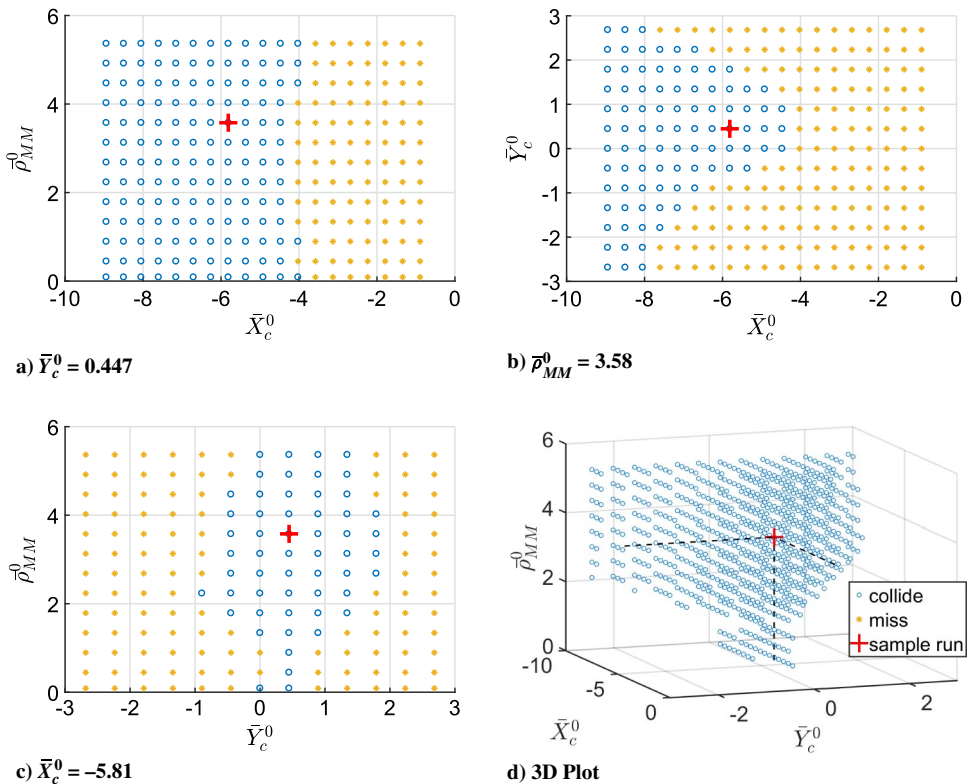


Fig. 6 Collision map. Data points where a missile hits its target were excluded in Fig. 6d for clarity.

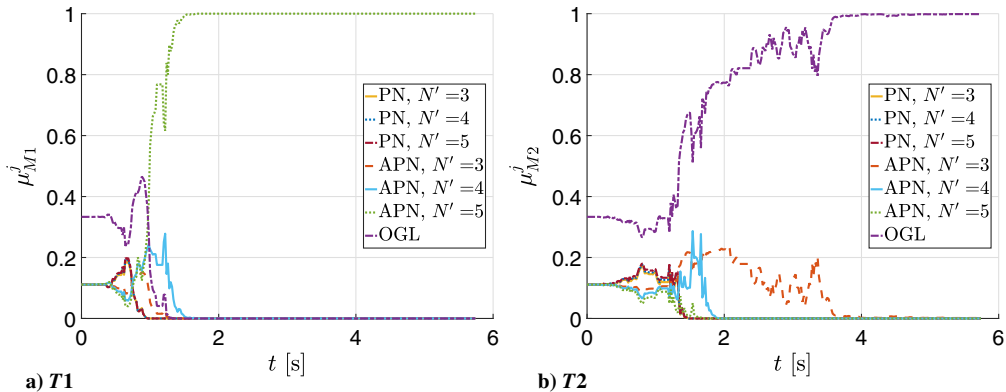


Fig. 7 Regime probabilities of  $T1$ 's and  $T2$ 's estimator.  $M1$  is using APN with  $N'_{APN} = 5$ , whereas  $M2$  is using OGL.

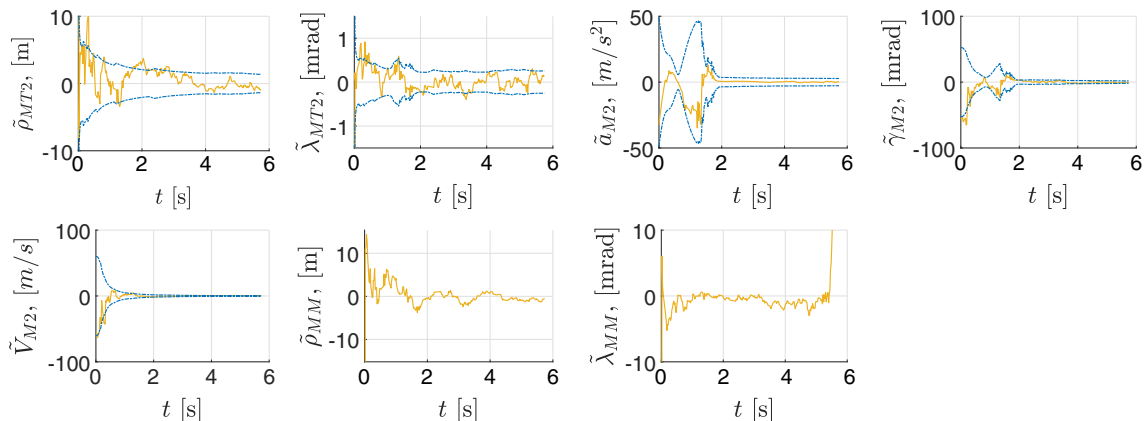


Fig. 8 Sample estimation error performance.

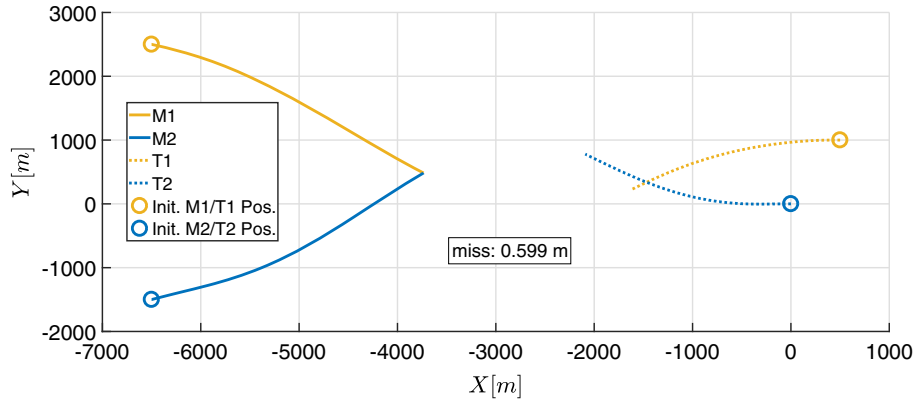


Fig. 9 Engagement trajectories when targets are using MMAC with M1 using APN,  $N'_{APN} = 5$ , and M2 using OGL.

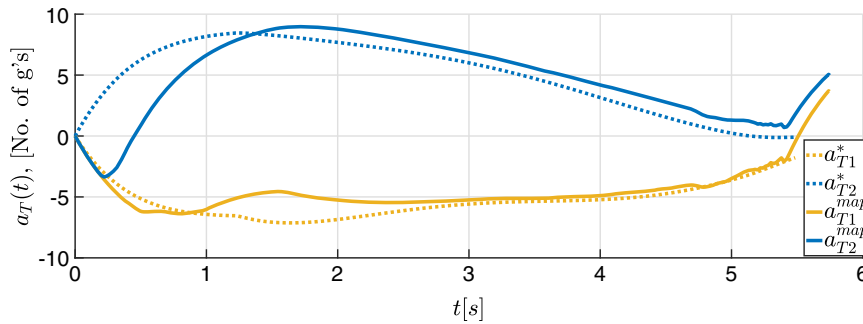


Fig. 10 Target acceleration profiles.

$$\mathbf{P}_{MTi}(k|k) = \sum_{j=1}^p \mu_i^j(k) [\mathbf{P}_{MTi}^j(k|k) + \bar{\mathbf{P}}_{MTi}^j] \quad (58b)$$

where  $\hat{\mathbf{x}}_{MTi}^j(k|k)$ ,  $j \in \{1, \dots, p\}$ , and  $\mathbf{P}_{MTi}^j(k|k)$  are the  $j$ th regime estimate and covariance of the  $i$ th estimator, respectively, and

$$\bar{\mathbf{P}}_{MTi}^j \triangleq [\hat{\mathbf{x}}_{MTi}^j(k|k) - \hat{\mathbf{x}}_{MTi}(k|k)][\hat{\mathbf{x}}_{MTi}^j(k|k) - \hat{\mathbf{x}}_{MTi}(k|k)]^T \quad (59)$$

Engagement trajectories of the sample run are shown in Fig. 9 and are very similar to what was depicted in Fig. 4b. Missile–missile miss distance in this run was 0.599 m. Acceleration profiles of the target pair in this sample run when using imperfect and perfect information (labeled  $a_{Ti}^{map}$  and  $a_{Ti}^*$ , respectively,  $i \in \{1, 2\}$ ) are plotted in Fig. 10. Initial disparities between  $a_{Ti}^{map}$  and  $a_{Ti}^*$  are observed due to large

estimation errors. As estimation errors converge at  $t \sim 2$  s,  $a_{Ti}^{map}$  behaves close to that of  $a_{Ti}^*$ . The kink observed in  $a_{Ti}^{map}$  near  $t = 5.4$  s was due to divergence of  $\tilde{\lambda}_{MM}$ , as observed in Fig. 8. The divergence is consistent with what was derived in Eq. (55), as  $\tilde{\lambda}_{MM}$  increases exponentially as  $\rho_{MM}$  approaches zero.

### 3. Monte Carlo Study

Results of the MC simulations are presented in this subsection. The performance metric in this study is the CDF of the miss distance between the missiles. The sensitivity of the miss CDF to measurement noise is evaluated here. Measurement noise variances are the same for both targets (i.e.,  $\sigma_{i,\rho} = \sigma_\rho$  and  $\sigma_{i,\lambda} = \sigma_\lambda$ , for  $i \in \{1, 2\}$ ). Figure 11 shows the CDF of the missile–missile miss distance for different levels of noise in the range and bearing measurements. As shown in Fig. 11, the miss CDF improves drastically with the reduction in  $\sigma_\rho$ . The results shown in Fig. 11

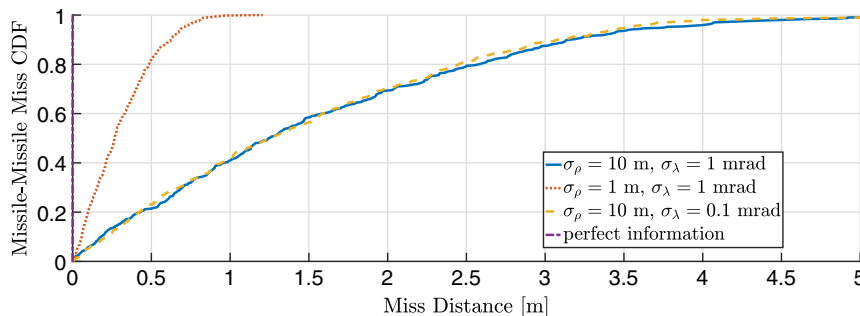


Fig. 11 Sensitivity of missile–missile miss distance to measurement noise.

substantiate the discussion in Sec. IV.E because the accuracy of the range estimates between the missile–target significantly affects the target pair’s ability to accurately nullify the missile–missile LOS and keep the pursuers on their collision triangle.

## VI. Conclusions

A novel optimal cooperative defensive strategy in a two-on-two engagement was derived in this paper. The proposed strategy capitalizes on the presence of multiple adversaries to lure them into collision. With the proposed multiple-model adaptive estimator (MMAE) scheme, the targets are able to identify the missiles’ guidance laws and predict their future trajectories. This information allows the target pair to maneuver cooperatively and set their pursuers on a collision triangle such that the missiles will hit each other before they could reach any of their targets.

of filters in the proposed decentralized scheme grows only linearly. The sensitivity of the proposed guidance law to the estimation error of the missile–target range was also presented analytically, and the findings were verified by Monte Carlo simulations.

Finally, it is important to note that the effectiveness of the guidance law also depends on the appropriate tuning of the weights in the cost function. Therefore, it is critical for the designer to make adjustments to the weights, if necessary, based on the required engagement conditions when applying the proposed guidance law.

## Appendix A: Definition of $A(t)$ and $B(t)$ in Equation (27)

Referring to Eq. (27), the submatrices in  $A(t)$  are defined as follows. The submatrix  $A_{MTi}$  represents the influence of the  $i$ th missile on the  $Mi$ – $Ti$  engagement:

$$A_{MTi} = \begin{bmatrix} 0 & 1 & [0] & [0] \\ -d_{Mi}K_1^{Mi} & -d_{Mi}K_2^{Mi} & -[C_{Mi} + d_{Mi}K_{Mi}] & C_{Ti} - d_{Mi}K_{Ti} \\ B_{Mi}K_1^{Mi} & B_{Mi}K_2^{Mi} & A_{Mi} + B_{Mi}K_{Mi} & B_{Mi}K_{Ti} \\ [0] & [0] & [0] & A_{Ti} \end{bmatrix}, \quad i \in \{1, 2\}$$

whereas  $A_{MM}^{Mi}$  represents the influence of the  $i$ th missile on the  $M1$ – $M2$  collision geometry:

$$A_{MM}^{M1} = \frac{1}{C_{MT1}^\delta} \begin{bmatrix} 0 & 0 & [0] & [0] \\ -C_{MM}^\delta d_{M1}K_1^{M1} & -C_{MM}^\delta d_{M1}K_2^{M1} & -C_{MM}^\delta [C_{M1} + d_{M1}K_{M1}] & -C_{MM}^\delta d_{M1}K_{T1} \\ d_{M1}K_1^{M1}/V_{M1} & d_{M1}K_2^{M1}/V_{M1} & [C_{M1} + d_{M1}K_{M1}]/V_{M1} & d_{M1}K_{T1}/V_{M1} \\ 0 & 0 & [0] & [0] \end{bmatrix},$$

$$A_{MM}^{M2} = \frac{1}{C_{MT2}^\delta} \begin{bmatrix} 0 & 0 & [0] & [0] \\ -C_{MM}^\delta d_{M2}K_1^{M2} & -C_{MM}^\delta d_{M2}K_2^{M2} & -C_{MM}^\delta [C_{M2} + d_{M2}K_{M2}] & -C_{MM}^\delta d_{M2}K_{T2} \\ 0 & 0 & [0] & [0] \\ -d_{M2}K_1^{M2}/V_{M2} & -d_{M2}K_2^{M2}/V_{M2} & -[C_{M2} + d_{M2}K_{M2}]/V_{M2} & -d_{M2}K_{T2}/V_{M2} \end{bmatrix}$$

When using perfect information, the proposed guidance strategy was shown to be effective over a wide range of initial conditions, as demonstrated by the collision map. This is despite the fact that the targets had half the maximum allowable acceleration and double the time lag compared to the missiles. This result highlights the advantage of the proposed cooperative strategy over conventional defensive strategies such as evasion or deploying defenders because the target pair was able to survive the engagement despite being less agile and not carrying any defending missiles.

For the case when the targets use imperfect information, a decentralized MMAC scheme was presented. Unlike the conventional MMAE approach, in which the number of required filters for guidance law identification grows quadratically with the number of possible missile guidance strategies, the number

and  $A_{MM}^0$  is defined as

$$A_{MM}^0 = \begin{bmatrix} A^0 & [0] \\ \Lambda_{MM} & [0] \end{bmatrix}$$

where  $A^0$  is

$$A^0 = \begin{bmatrix} 0 & 1 \\ 0 & 0 \end{bmatrix}$$

and  $\Lambda_{MM}$  consist of terms associated with  $\lambda_{MM}$ :

$$\Lambda_{MM} = \frac{1}{V_{C,MM}t_{go,MM}^2} \begin{bmatrix} -1 & -t_{go,MM} \\ 1 & t_{go,MM} \end{bmatrix}$$

Next, we define  $\mathbf{B}(t)$ . Submatrix  $\mathbf{B}_{MTi}$  describes the influence of the  $i$ th target on the  $Mi$ - $Ti$  engagement:

$$\mathbf{B}_{MTi} = \begin{bmatrix} 0 & d_{Ti} - d_{Mi}K_{u_{Ti}} & K_{u_{Ti}}\mathbf{B}_{Mi}^T & \mathbf{B}_{Ti}^T \end{bmatrix}^T, \quad i \in \{1, 2\}$$

and submatrices  $\mathbf{B}_{MM}^{Ti}$ ,  $i \in \{1, 2\}$ , represent the influence of the  $i$ th target on the  $M1$ - $M2$  collision geometry:

$$\mathbf{B}_{MM}^{T1} = \frac{1}{C_{MT1}^\delta} \begin{bmatrix} 0 & -C_{MM}^\delta d_{M1}K_{u_{T1}} & d_{M1}K_{u_{T1}}/V_{M1} & 0 \end{bmatrix}^T$$

$$\mathbf{B}_{MM}^{T2} = \frac{1}{C_{MT2}^\delta} \begin{bmatrix} 0 & -C_{MM}^\delta d_{M2}K_{u_{T2}} & 0 & -d_{M2}K_{u_{T2}}/V_{M2} \end{bmatrix}^T$$

### Acknowledgment

This effort was sponsored by the U.S. Air Force Office of Scientific Research, Air Force Materiel Command, under grant FA9550-15-1-0429. The U.S. Government is authorized to reproduce and distribute reprints for Governmental purpose notwithstanding any copyright notation thereon.

### References

- [1] Nigam, N., and Kroo, I., "Control and Design of Multiple Unmanned Air Vehicles for a Persistent Surveillance Task," *12th AIAA/ISSMO Multidisciplinary Analysis and Optimization Conference*, AIAA Paper 2008-5913, Sept. 2008. doi:10.2514/6.2008-5913
- [2] Ousingsawat, J., and Campbell, M. E., "Optimal Cooperative Reconnaissance Using Multiple Vehicles," *Journal of Guidance, Control, and Dynamics*, Vol. 30, No. 1, 2007, pp. 122–132. doi:10.2514/1.19147
- [3] Jeon, I.-S., Lee, J.-I., and Tahk, M.-J., "Homing Guidance Law for Cooperative Attack of Multiple Missiles," *Journal of Guidance, Control, and Dynamics*, Vol. 33, No. 1, 2010, pp. 275–280. doi:10.2514/1.40136
- [4] Earl, M. G., and D'Andrea, R., "A Decomposition Approach to Multi-Vehicle Cooperative Control," *Robotics and Autonomous Systems*, Vol. 55, No. 4, 2007, pp. 276–291. doi:10.1016/j.robot.2006.11.002
- [5] Isaacs, R., *Differential Games*, Wiley, New York, 1965, pp. 336–356.
- [6] Ho, Y., Bryson, A., and Baron, S., "Differential Games and Optimal Pursuit–Evasion Strategies," *IEEE Transactions on Automatic Control*, Vol. 10, No. 4, 1965, pp. 385–389. doi:10.1109/TAC.1965.1098197
- [7] Breakwell, J. V., and Merz, A. W., "Minimum Required Capture Radius in a Coplanar Model of the Aerial Combat Problem," *AIAA Journal*, Vol. 15, No. 8, 1977, pp. 1089–1094. doi:10.2514/3.7399
- [8] Battistini, S., and Shima, T., "Differential Games Missile Guidance with Bearings-Only Measurements," *IEEE Transactions on Aerospace and Electronic Systems*, Vol. 50, No. 4, 2014, pp. 2906–2915. doi:10.1109/TAES.2014.130366
- [9] Borg, D. A., and Julich, P. M., "Proportional Navigation vs an Optimally Evading, Constant-Speed Target in Two Dimensions," *Journal of Spacecraft and Rockets*, Vol. 7, No. 12, 1970, pp. 1454–1457. doi:10.2514/3.30190
- [10] Slater, G. L., and Wells, W., "Optimal Evasive Tactics Against a Proportional Navigation Missile with Time Delay," *Journal of Spacecraft and Rockets*, Vol. 10, No. 5, 1973, pp. 309–313. doi:10.2514/3.27759
- [11] Shinar, J., and Steinberg, D., "Analysis of Optimal Evasive Maneuvers Based on a Linearized Two-Dimensional Kinematic Model," *Journal of Aircraft*, Vol. 14, No. 8, 1977, pp. 795–802. doi:10.2514/3.58855
- [12] Ben-Asher, J. Z., and Cliff, E. M., "Optimal Evasion Against a Proportionally Guided Pursuer," *Journal of Guidance, Control, and Dynamics*, Vol. 12, No. 4, 1989, pp. 598–600. doi:10.2514/3.20450
- [13] Shima, T., "Optimal Cooperative Pursuit and Evasion Strategies Against a Homing Missile," *Journal of Guidance, Control, and Dynamics*, Vol. 34, No. 2, 2011, pp. 414–425. doi:10.2514/1.51765
- [14] Shaferman, V., and Shima, T., "Cooperative Multiple-Model Adaptive Guidance for an Aircraft Defending Missile," *Journal of Guidance, Control, and Dynamics*, Vol. 33, No. 6, 2010, pp. 1801–1813. doi:10.2514/1.49515
- [15] Fonod, R., and Shima, T., "Multiple Model Adaptive Evasion Against a Homing Missile," *Journal of Guidance, Control, and Dynamics*, Vol. 39, No. 7, 2016, pp. 1578–1592. doi:10.2514/1.G000404
- [16] Magill, D., "Optimal Adaptive Estimation of Sampled Stochastic Processes," *IEEE Transactions on Automatic Control*, Vol. 10, No. 4, 1965, pp. 434–439. doi:10.1109/TAC.1965.1098191
- [17] Lainiotis, D. G., "Partitioning: A Unifying Framework for Adaptive Systems, 2: Control," *Proceedings of the IEEE*, Vol. 64, No. 8, 1976, pp. 1182–1198. doi:10.1109/PROC.1976.10289
- [18] Ratnoff, A., and Shima, T., "Line-of-Sight Interceptor Guidance for Defending an Aircraft," *Journal of Guidance, Control, and Dynamics*, Vol. 34, No. 2, 2011, pp. 522–532. doi:10.2514/1.50572
- [19] Kumar, S. R., and Shima, T., "Cooperative Nonlinear Guidance Strategies for Aircraft Defense," *Journal of Guidance, Control, and Dynamics*, Vol. 40, No. 1, 2017, pp. 124–138. doi:10.2514/1.G000659
- [20] Zarchan, P., *Tactical and Strategic Missile Guidance*, AIAA, Reston, VA, 2012, Chap. 2. doi:10.2514/4.868948
- [21] Garber, V., "Optimum Intercept Laws for Accelerating Targets," *AIAA Journal*, Vol. 6, No. 11, 1968, pp. 2196–2198. doi:10.2514/3.4962
- [22] Cottrell, R. G., "Optimal Intercept Guidance for Short-Range Tactical Missiles," *AIAA Journal*, Vol. 9, No. 7, 1971, pp. 1414–1415. doi:10.2514/3.6369
- [23] Bryson, A., and Ho, Y., *Applied Optimal Control: Optimization, Estimation and Control*, Taylor and Francis, New York, 1975, pp. 146–152.
- [24] Friedland, B., *Advanced Control System Design*, Prentice–Hall, Upper Saddle River, NJ, 1996, pp. 110–112.
- [25] Tahk, M.-J., Ryoo, C.-K., and Cho, H., "Recursive Time-to-Go Estimation for Homing Guidance Missiles," *IEEE Transactions on Aerospace and Electronic Systems*, Vol. 38, No. 1, 2002, pp. 13–24. doi:10.1109/7.993225
- [26] Bar-Shalom, Y., and Li, X.-R., *Estimation with Applications to Tracking and Navigation*, Wiley, New York, 2001, Chap. 11.
- [27] Oshman, Y., Shinar, J., and Weizman, S. A., "Using a Multiple-Model Adaptive Estimator in a Random Evasion Missile/Aircraft Encounter," *Journal of Guidance, Control, and Dynamics*, Vol. 24, No. 6, 2001, pp. 1176–1186. doi:10.2514/2.4833